Journal of Groundwater Science and Engineering
ISSN 2305-7068
Indexed by ESCI CABI CSA
Scopus GeoRef AJ CNKI

Variation characteristics of CO_2 in a newly-excavated soil profile, Chinese Loess Plateau: Excavation-induced ancient soil organic carbon decomposition

Chao Song, Man Liu, Qiu-yao Dong, Lin Zhang, Pan Wang, Hong-yun Chen, Rong Ma

Citation:
Song C, Liu M, Dong QY, *et al*. 2022. Variation characteristics of CO_2 in a newly-excavated soil profile, Chinese Loess Plateau: Excavation-induced ancient soil organic carbon decomposition. Journal of Groundwater Science and Engineering, 10(1): 19-32.

View online: https://doi.org/10.19637/j.cnki.2305-7068.2022.01.003

Journal homepage: http://gwse.iheg.org.cn

Variation characteristics of CO_2 in a newly-excavated soil profile, Chinese Loess Plateau: Excavation-induced ancient soil organic carbon decomposition

Chao Song[1,2], Man Liu[3], Qiu-yao Dong[1,2*], Lin Zhang[1,2], Pan Wang[1,2], Hong-yun Chen[1,2], Rong Ma[4]

[1] *Institute of Hydrogeology and Environmental Geology, Chinese Academy of Geological Sciences, Shijiazhuang* 050061, *China*.
[2] *Key Laboratory of Quaternary Chronology and Hydro-Environmental Evolution, China Geological Survey, Shijiazhuang* 050061, *China*.
[3] *Institute of Earth Sciences, China University of Geosciences (Beijing), Beijing* 100083, *China*.
[4] *State Key Laboratory of Hydrology-Water Resources and Hydraulic Engineering, Nanjing Hydraulic Research Institute, Nanjing* 210029, *China*.

Abstract: Soils of the Chinese Loess Plateau (CLP) contain substantial amounts of soil inorganic carbon (SIC), as well as recent and ancient soil organic carbon (SOC). With the advent of the Anthropocene, human perturbation, including excavation, has increased soil CO_2 emission from the huge loess carbon pool. This study aims to determine the potential of loess CO_2 emission induced by excavation. Soil CO_2 were continuously monitored for seven years on a newly-excavated profile in the central CLP and the stable C isotope compositions of soil CO_2 and SOC were used to identify their sources. The results showed that the soil CO_2 concentrations ranged from 830 $\mu L \cdot L^{-1}$ to 11 190 $\mu L \cdot L^{-1}$ with an annually reducing trend after excavation, indicating that the human excavation can induce CO_2 production in loess profile. The $\delta^{13}C$ of CO_2 ranged from –21.27 ‰ to –19.22 ‰ (mean: –20.11‰), with positive deviation from top to bottom. The range of $\delta^{13}C_{SOC}$ was –24.0‰ to –21.1‰ with an average of –23.1‰. The $\delta^{13}C$-CO_2 in this study has a positive relationship with the reversed CO_2 concentration, and it is calculated that 80.22% of the soil CO_2 in this profile is from the microbial decomposition of SOC and 19.78% from the degasification during carbonate precipitation. We conclude that the human excavation can significantly enhance the decomposition of the ancient OC in loess during the first two years after perturbation, producing and releasing soil CO_2 to atmosphere.

Keywords: Soil organic matter; Human excavation; Soil CO_2; Stable carbon isotopic composition; China Loess Plateau

Received: 20 Mar 2021/ Accepted: 25 Dec 2021

Introduction

Global mean temperature has risen 1.1℃ since pre-industrial times and is predicted to increase further by 1.5-4.4℃ according to the IPCC (Intergovernmental Panel on Climate Change) sixth Assessment Report in 2021, due to increasing emission of CO_2 and other greenhouse gases (IPCC, 2021). Soil organic carbon (SOC) stock, as the largest carbon pool in the terrestrial biosphere, stores 615 Gt SOC in the top 0.2 m layer and 2 344 Gt SOC at depth of up to 3 m, the amount of which is more than the combined CO_2 in both biomass and atmosphere (Jobbágy and Jackson, 2000; Fontaine et al. 2007), and has received a lot of attention recently due to its ability to influence atmospheric CO_2 concentrations (Lal, 2004; IPCC, 2018; Han et al. 2020). In contrast to the great progress made in understanding the dynamics of the SOC pool, soil inorganic carbon (SIC) has been less studied, although the degasification during carbonate precipitation can also release large amount of CO_2 (Zamanian et al. 2018; Liu and Han, 2020). In fact, in arid and semiarid regions, SIC, rather than SOC, is the dominant form of carbon, with a reservoir approximately 2-10 times larger than that of SOC

*Corresponding author: Qiu-yao Dong, *E-mail address*: dongqiuyao@mail.cgs.gov.cn

DOI: 10.19637/j.cnki.2305-7068.2022.01.003

Song C, Liu M, Dong QY, et al. 2022. Variation characteristics of CO_2 in a newly-excavated soil profile, Chinese Loess Plateau: Excavation-induced ancient soil organic carbon decomposition. Journal of Groundwater Science and Engineering, 10(1): 19-32.

(Tan et al. 2014). A subtle fluctuation of SIC pool can strongly alter the regional carbon budget in arid and semiarid areas (Gao et al. 2017).

In the semiarid region of North China, Chinese Loess Plateau (CLP) has huge soil carbon storage consisting of 197 Gt SOC (Qin et al. 2001) and 850 Gt SIC (Liu et al. 2001). Due to its thickness (up to 200 m) (Liu, 1985), the subsoil carbon pools in the CLP may be of major importance. The SOC pool in subsoil or deep soil of the CLP consists of paleovegetation-originated substrate-inherent OC with different ages from thousands to millions of years, which mainly accumulated in paleosol layers when the loess-paleosol sequences were formed in glacial-interglacial cycle (Liu et al. 2007). While SOC stored at depth is generally stable, it may be subject to cycling if biological and physicochemical processes contributing to its protection are changing (Chaopricha and Marín-Spiotta, 2014). In the CLP, the huge carbon stocks in deep loess is commonly exposed to air by natural erosion and/or human perturbations such as engineering excavation and terracing practices (Chen et al. 2020). As a result, the old substrate-inherent OC may be decomposed by microbial and consequently produce CO_2 in the pore of soil because of the exposure of initially protected SOC (Pabst et al. 2016; Chen et al. 2020), further result in a lateral carbon flux via the excavating profile (Song et al. 2017a; 2017b). According to the estimation from Song (2017) on terracing practices in a small studied area in the southeast of Qiushe, the exposed vertical area of back wall in the terracing accounts for roughly 50% of the horizontal area in the study region, and the lateral CO_2 flux through the vertical back wall occupies 20% of the vertical CO_2 flux from the surface. Thus the lateral carbon flux via loess excavating profile is a neglected but important carbon flux. The increase in soil CO_2 would result in the precipitation of carbonate in the alkaline environment (Wang et al. 2015; Zamanian et al. 2016; Gao et al. 2017), and on the other hand, may dissolve carbonate mineral, leading to the vertical movement of SIC as dissolve inorganic carbon (DIC) to subsoil or deeper soil (Liu, 2011; Gerke et al. 2015), or discharge to riverine system via the spring water or well water extraction.

Soil CO_2 as an observable proxy is directly linked to these processes (Pabst, et al. 2016; Song, et al. 2017a). Several researchers have reported CO_2 concentration in soils of the CLP ranging from 740 μL/L to 19 600 μL/L in Weinan, with $\delta^{13}C\text{-}CO_2$ varying from −12.01 ‰ to −1.94 ‰ (Liu et al. 1997). Similar CO_2 concentration observations were recorded in Puxian, ranging from 1 312.9 μL/L to 5 945.5 μL/L with a trend to higher CO_2 concentration in paleosol layers than in adjacent loess layers, with $\delta^{13}C\text{-}CO_2$ values between −15.48‰ to −11.14‰ (Liu et al. 2001), suggesting that the CO_2 emissions were related to two processes: microbial decomposition of stable organic matter and the degassing effect of carbonates (Song et al. 2017a; 2017b). However, the importance of these two processes through time has not yet been addressed.

We hypothesised that the primary equilibrium of the ancient soil carbon will be disrupted when soils are subjected to disturbance or stress, and that this disruption and its prime effect on soil carbon can be observed by soil CO_2 variations. Therefore, in order to further understand the vulnerability of SOC and SIC in deep ancient loess after human excavation and thus exposure to the atmosphere, we monitored CO_2 concentration for seven -years on a newly-excavated loess profile with an age of roughly 2.0 Ma B.P. analysed the amount and characteristics of CO_2 concentration and investigated the origin of CO_2 using stable carbon isotopic composition of SOC and CO_2 in this study.

1 Study area and soil profile

The study area is located in Lingtai County (107°41′ E, 35°10′ N), Pingliang city, Gansu Province, in northern China (Fig. 1), where the type of climate is a semi-humid, warm temperate, continental monsoon climate, characterized by relatively hot, humid summers and cold, dry winters. The mean temperature is 15.3℃, with monthly mean temperature in July and January of 22.1℃ and −4.7℃, respectively. Mean annual precipitation is 605.5 mm, with rainfall concentrating mainly in the summer and autumn. Mean annual latent evaporation reaches to 1 492 mm.

The soil profile LTC in this study was excavated in March of 2013 for building construction, forming a fresh outcrop of ancient loess with a depth of more than 8 m. The age of aeolian deposit were estimated roughly 2.0 Ma B.P. based on the on-site survey of loess sequences and the laboratory analysis of magnetic susceptibility and grain size data. Another loess section we studied previously in Qiushe village, Dudian Town, Lingtai County (QS section) can be regarded as a parallel profile for verification (Song et al. 2017a; 2017b). The distance between QS and LTC section is only 25 km.

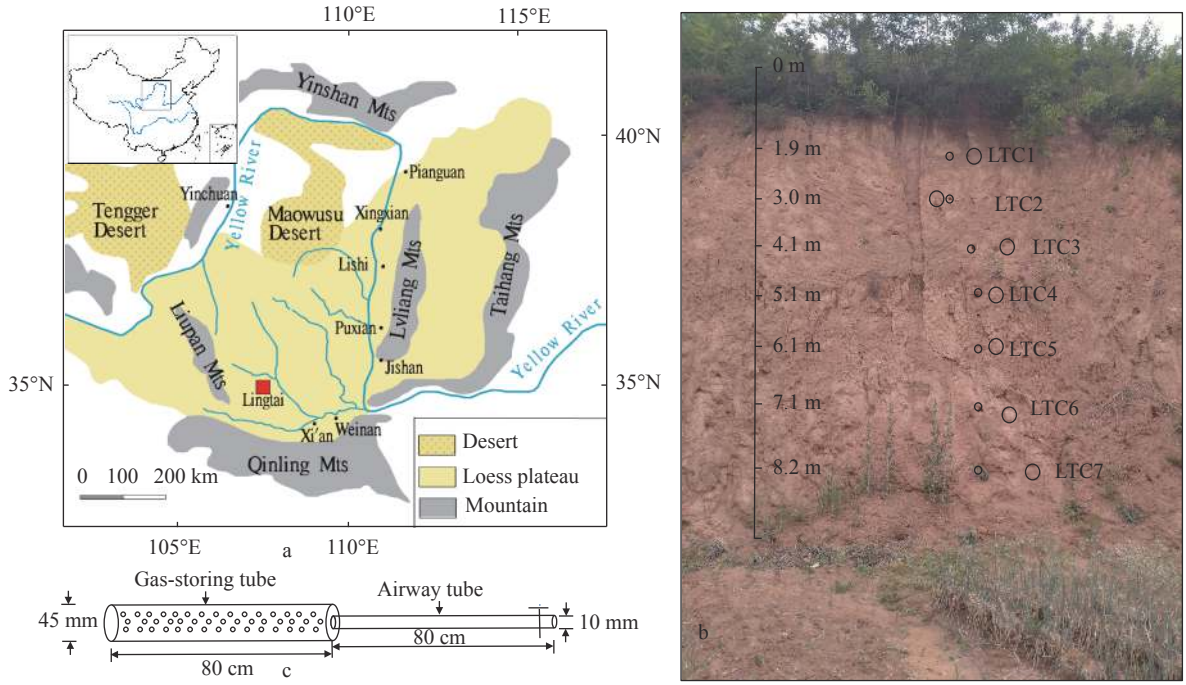

Fig. 1 The location map of study area (a), the studied section (b) and the sketch map of the tube for gas monitoring and sampling (c)

(a) Chinese Loess plateau: Red square- The location of the study area; (b) the loess section for gas monitoring: Small circle is the location of gas concentration monitoring and gas sampling inside soil; big circles are the locations for monitoring the lateral gases flux out of loess section; (c) the tubes for gas monitoring and sampling which were buried inside loess (see small circles in Fig.1b): Gas-storing tube: L=80 cm, Ø=45 mm; airway tube: L=80 cm, Ø=10 mm

2 Methods

2.1 Soil sampling, pre-treatment and analysis

The soil samples were taken at 2 cm interval in the soil profile. A total of 355 samples were collected. All samples were air-dried, and sieved to pass a 2-mm mesh. Visible roots were removed. An aliquot was ground to pass a 0.25-mm mesh for total soil organic carbon (TOC) determination. A 5-g sample of air-dried soil (<0.25 mm) was placed in a 100-mL centrifuge tube and treated with 0.5 mol·L^{-1} HCl for 24 h to remove carbonate, then the suspension was centrifuged at 3 000 rpm for 10 min and decanted after centrifugation. The soil remaining in the centrifuge tube was rinsed repeatedly with distilled water until the removed rinse water was neutral. Finally, the residue (carbonate-free soil) was dried at 40℃ for 48 h, and ground to pass a 149-μm sieve for SOC determination. The organic carbon content and soil total carbon was analyzed by combustion using a multi-element analyzer (vario TOC cube, Elementar, Germany) with a precision of ≤0.1%. Soil inorganic carbon (SIC) was calculated as the difference between TC (total carbon) and SOC (Liu et al. 2021). The $\delta^{13}C$ of SOC was analyzed using the MAT-253 gas mass spectrometer with a dual inlet system. Carbon isotopic ratios in samples are expressed as per mil deviation (VPDB standard), with a precision of ±0.1‰ or better.

2.2 Observation of gases in soil

2.2.1 On-site observation of soil CO_2 concentration

Seven horizontal monitoring holes at 1.9 m, 3.0 m, 4.1 m, 5.1 m, 6.1 m, 7.1 m, and 8.2 m depths were drilled in this soil profile by using a handheld electrical drilling machine (Fig. 1) in January, 2014, and PPR (polypropylene random) tubes (gas-storing tube: L=80 cm, Ø=45 mm; airway tube: L=80 cm, Ø=10 mm) were buried in each hole and fitted at the exit with a stoppered female end of a plastic union to observe the concentration of CO_2 and to collect the gaseous samples. The concentration of soil CO_2 was measured with the ATX620 meter (Industrial Scientific Corp, Oakdale, PA, USA) for ten times: In February, March, April and June of 2014, February, April, and May of 2015, February and October of 2017, September of 2019 and June of 2020, where February represents

winter season, March and April for spring, May and June for summer, and September and October for autumn. The resolution is 10 μL/L.

2.2.2 CO_2 efflux

At each depth, the lateral efflux of CO_2 through the soil profile was measured by the WEST System portable soil flux meter (West Systems S.r.l., Italy). The meter is based on the accumulation chamber technique and has been widely used to quantify diffuse soil degassing of carbon dioxide and other gas species (Granieri et al. 2003; Capaccioni et al. 2011; Popiţa et al. 2015; Liegler 2016). The system consists of an accumulation closed-chamber 20 cm high with a surface of 314 cm^2, an LI-840A CO_2/H_2O detector to measure CO_2 and water vapor (CO_2: A range of 0-20 000 μL/L and an analytical accuracy of 2%; H_2O: A range of 0-60 mmol/mol and an analytical accuracy of 1.5%), an TDLAS (Tunable Diode Laser Absorption Spectroscopy) CH_4 detector (range 0.1 μL/L - 100% vol., analytical accuracy 10%, resolution 0.1 μL/L), and wireless data communication to a palm-top computer. The chamber is then equipped with a Nafion dryer for humidity removal and an internal fan to assure mixing of gas inside it. The gas fluxes are automatically calculated through a linear regression of the gas concentration build-up in the chamber.

In order to measure the lateral efflux of CO_2 and other gases, we developed a cutting ring with the same size as the chamber to seal the gap between the chamber and the observed soil profile. Before determination, we used the tool to carve an annular groove, and the chamber was sealed from any leakage with an attached hand-made collar by rubber. The CO_2 efflux was observed in October 2015, May 2016, and February 2017.

2.2.3 Sampling of soil CO_2 and the measurement of $\delta^{13}C$-CO_2

In order to investigate the origin and controlling factors of soil CO_2, the gaseous samples were collected into gas sampling bags in field and sent to the Institute of Earth Environment, Chinese Academy of Sciences. The CO_2 was cryogenically purified and analyzed using the MAT-251 gas mass spectrometer with a dual inlet system. Carbon isotopic ratios in samples are expressed as per mil deviation, relative to the VPDB standard, with a precision of ±0.2‰ or better.

3 Results

3.1 Concentration of soil CO_2 and its $\delta^{13}C$

The CO_2 concentration in the soil profile is presented in Table 1. The results showed that the CO_2 concentration in soil ranged from 830 $\mu L \cdot L^{-1}$ to 11 190 $\mu L \cdot L^{-1}$, which was twice to twelve times higher than that in the atmosphere (roughly 410 $\mu L \cdot L^{-1}$). According to Table 2, the CO_2 concentrations decrease with depth. We also observed a seasonal variation of the concentration of CO_2 — the concentrations decreased in this order: Summer >fall ≈ spring >winter (Fig. 2), indicating their dependence on air temperature. However, in 2014, CO_2 in soil had a high concentration at the beginning of the profile formation and showed a decreasing trend, followed by an increase (Fig. 2).

Table 1 Concentration of CO_2

No.	Depth/m	2014Feb.	2014Mar.	2014Apr.	2014 Jun.	2015Feb.	2015Oct.	2016May	2017Feb.	2019Sept.	2020June
Temp.	-	6℃	14℃	16℃	26℃	9℃	20℃	22℃	5℃	21℃	25℃
In air	-	410	430	410	410	410	390	410	410	410	410
LTC1	1.9	5 740	4 350	5 740	11 190	2 520	4 810	3 760	1 130	4 130	4 110
LTC2	3.1	3 540	3 430	3 890	4 810	2 240	4 240	2 870	1 130	2 150	2 670
LTC3	4.1	3 090	2 930	3 320	4 170	1 970	3 400	2 670	1 540	2 990	2 300
LTC4	5.2	2 370	2 310	2 720	3 650	1 380	2 530	2 060	1 180	2 410	1 880
LTC5	6.1	2 560	2 270	2 630	3 340	1 340	2 300	1 760	1 130	2 230	1 920
LTC6	7.1	2 340	2 200	2 450	3 030	1 190	1 930	1 780	830	2 650	1 670
LTC7	8.2	1 440	2 700	N.d.	N.d.	N.d.	N.d.	N.d.	N.d.	N.d.	N.d.

N.d.=no data. The monitoring tube of LTC7 was destroyed since April of 2014.

Table 2 Results of the efflux of CO_2 and water vapor

Depth/m		CO_2 /g·m^{-2}·d^{-1}			H_2O /g·m^{-2}·d^{-1}		
D. T.		Oct., 2015	May, 2016	Feb., 2017	Oct., 2015	May, 2016	Feb., 2017
Temp.(Weather)		20℃ (Cloudy)	22℃ (Sunny)	5℃(Sunny)	20℃ (Cloudy)	22℃ (Sunny)	5℃(Sunny)
Surface	0.0	11.53	16.02	3.48	112.14	155.88	182.16
LTC1	1.9	0.47	18.83	2.91	15.36	56.74	4.85
LTC2	3.0	1.42	2.30	0.14	3.83	64.89	62.17
LTC3	4.1	1.31	1.20	0.47	41.38	216.90	8.12
LTC4	5.1	0.32	2.96	0.07	83.05	172.76	5.08
LTC5	6.1	2.99	2.72	0.54	21.17	361.26	76.07
LTC6	7.1	0.84	5.02	0.37	18.63	390.06	87.23
LTC7	8.2	3.86	2.75	0.32	264.60	386.46	229.32
Mean	-	1.60	5.11	0.69	64.00	235.58	67.55

D. T.=determination time; All the observations were done at 10:00 a. m. of the set testing date. Mean=the average value of these 7 observed results in the LTC profile.

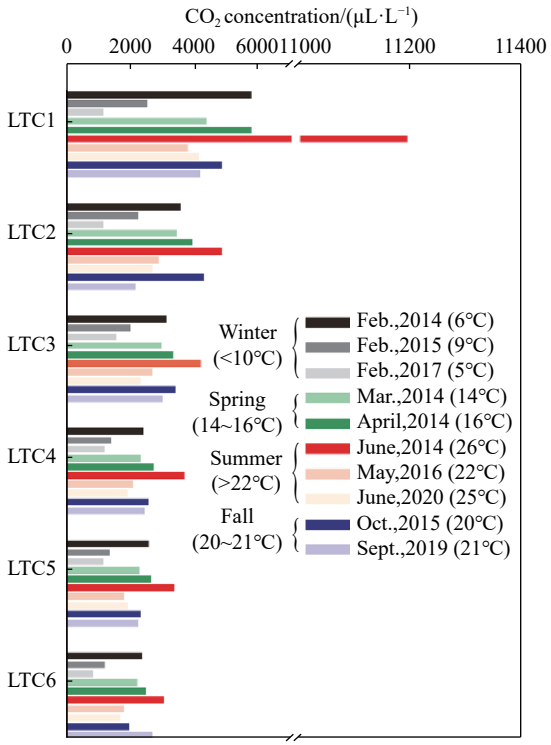

Fig. 2 Variation of soil CO_2 concentration in different season

The concentrations of CO_2 displayed a decreasing trend with time (Fig. 2), which was observed from the single result of February 2014, 2015 and 2017, e.g. from 5 740 μL·L^{-1} in Feb 2014 to 1 130 μL·L^{-1} in Feb 2017 at LTC1, from 2 340 μL·L^{-1} to 830 μL·L^{-1} at LTC6 (Table 1), despite decrease in the reduction extent with depth (Fig. 2). In summer, the CO_2 concentration decreased from 3 030-11 190 μL·L^{-1} in June 2014 to 1 670-4 110 μL·L^{-1} in June 2020 (see Table 1). Moreover, the temperature in May 2016 was higher than in March and April, 2014, but the CO_2 concentration had lower values in May 2016 than in March and April of 2014 (Fig. 2). These also indicated that CO_2 concentration in this profile had an annual decline after excavation.

The $\delta^{13}C$ of CO_2 ranged from –21.27 ‰ to –19.22 ‰ with an average of –20.11‰, with negative deviation following by positive deviation from top to bottom, displaying a negative relationship with CO_2 concentration (Fig. 3).

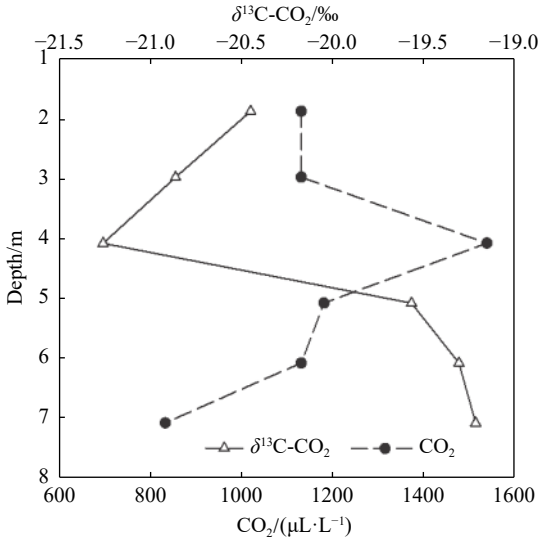

Fig. 3 Concentration and $\delta^{13}C$ of CO_2 at LTC profile in February, 2017

3.2 Gas efflux of CO_2, CH_4 and H_2O

The diffuse carbon dioxide efflux ranged from 0.32 g·m^{-2}·d^{-1} to 3.84 g·m^{-2}·d^{-1} (1.60 on average) through lateral verses 11.53 g·m^{-2}·d^{-1} on the surface in October 2015, from 1.20 g·m^{-2}·d^{-1} to 18.83 g·m^{-2}·d^{-1} (5.11 on average) verses 16.02

$g \cdot m^{-2} \cdot d^{-1}$ in May 2016, and from 0.07 $g \cdot m^{-2} \cdot d^{-1}$ to 2.91 $g \cdot m^{-2} \cdot d^{-1}$ (0.69 on average) verses 3.48 $g \cdot m^{-2} \cdot d^{-1}$ in February 2017, respectively (Table 2). The results showed that the CO_2 efflux in summer were higher than that in winter, and had a decreasing trend with depth (Table 2). The diffuse efflux of H_2O was 3.83-264.60 $g \cdot m^{-2} \cdot d^{-1}$ (64.00 on average) through lateral verses 112.14 $g \cdot m^{-2} \cdot d^{-1}$ on the surface in October 2015, 56.74-390.06 $g \cdot m^{-2} \cdot d^{-1}$ (235.58 on average) vs. 155.88 $g \cdot m^{-2} \cdot d^{-1}$ in May 2016, and 4.85-229.32 $g \cdot m^{-2} \cdot d^{-1}$ (67.55 on average) vs. 182.16 $g \cdot m^{-2} \cdot d^{-1}$ in February 2017, respectively (Table 2), showing a higher efflux in summer than winter, but no distinct trend with depth or time was observed (Table 2). No methane efflux above the detection limit was found.

3.3 SOC, SIC and $\delta^{13}C_{SOC}$

Fig. 4 shows the results of soil organic carbon (SOC, %) and soil inorganic carbon (SIC, %) and $\delta^{13}C_{SOC}$ in the LTC profile. SOC varied from 0.04%-0.28% with an average of 0.07%. Except the maximum was found at the top of this profile, SOC showed a concentrated range of 0.04%-0.11%, with a slight enhancement at the depth of 6.4-7.4 m (Fig. 4). The SIC value ranged from 0.59%-3.13% with an average of 1.78%. A distinct high value of SIC was observed at the depth of 5.2-6.4 m in this profile. The range of $\delta^{13}C_{SOC}$ was –24.0‰- –21.1‰ with an average of–23.1‰, exhibiting the highest carbon isotope composition (–21.1 ‰) at the depth of 6.8 m. According to Fig. 4, there are no extreme values of SOC, SIC and $\delta^{13}C_{SOC}$ at the positions with gas monitoring tube (LTC1-LTC6 in Fig. 4). Fig. 5 and Fig. 6 indicated that the $\delta^{13}C_{SOC}$ had a positive relationship with SOC (R^2=0.33) while a negative relationship with SIC carbon (R^2=0.16), suggesting that the SOC had been strongly decomposed and consequently part of them had been transformed to SIC (Chen et al. 2007).

4 Discussion

4.1 Characteristics and origin of soil CO_2

The CO_2 concentrations in LTC profile range from 830 $\mu L \cdot L^{-1}$ to 11 900 $\mu L \cdot L^{-1}$ (Mean = 2 823 $\mu L \cdot L^{-1}$ and n = 62), which are similar to the results from other loess profiles, e.g. 550-6 970 $\mu L \cdot L^{-1}$ (mean= 2 237 $\mu L \cdot L^{-1}$ and n=132) in QS loess profile of Lingtai (Song et al. 2017b) and 1 313-5 946 $\mu L \cdot L^{-1}$

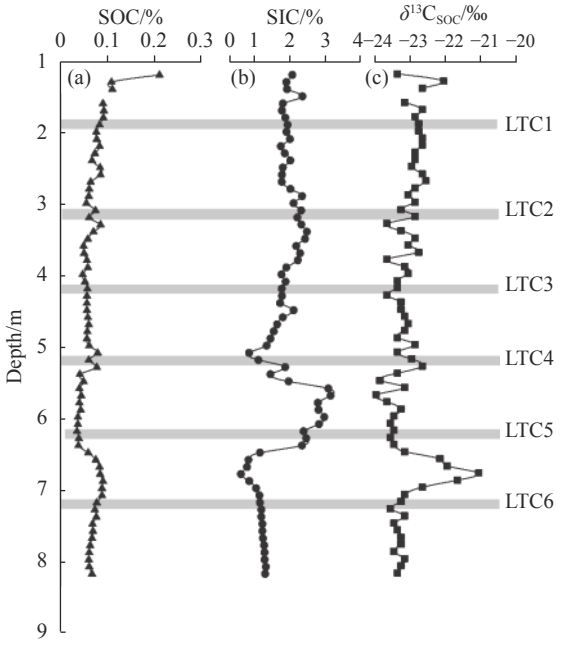

Fig. 4 Variation characteristics of total organic carbon (SOC), total inorganic carbon (SIC) and $\delta^{13}C_{SOC}$ with depth

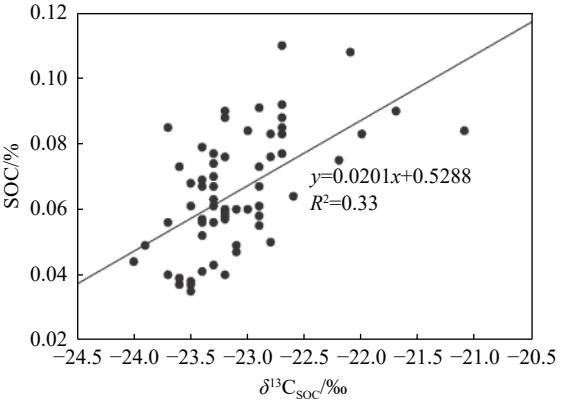

Fig. 5 Relationship between SOC (%) and $\delta^{13}C_{SOC}$ (‰) (P<0.05)

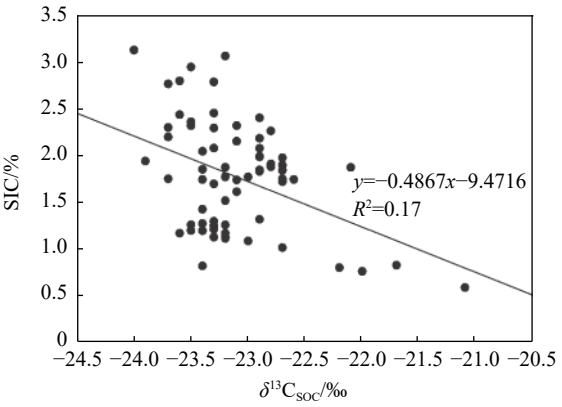

Fig. 6 Relationship between SIC (%) and $\delta^{13}C_{SOC}$ (‰) (P <0.05)

(mean=3 301 μL·L^{-1} and n=19) in Puxian loess profile (Liu et al. 2001), except the anomalous high value (11 900 μL·L^{-1}) at LTC 1 within the first two years after excavation. The results are also within the range of concentrations reported from other field observations (Keller and Bacon, 1998; Thorstenson et al. 1998; Etiope, 1999; Hendry et al. 1999; Walvoord et al. 2005), but much less than the maximum values reported near the water table in unsaturated zones (Wood and Petraitis, 1984; Suchomel et al. 1990; Etiope, 1999; Arora et al. 2016). The range of δ^{13}C-CO$_2$ in this loess profile (−21.27 ‰ - −19.22 ‰ with an average of −20.11 ‰) is slightly lower than the range of −21.31‰ to −15.37‰ in the nearby QS loess section of Lingtai County (Song et al. 2017a), but much lower than the range of −15.48 ‰ - −11.14 ‰ in a far-away Puxian section of Shanxi Province (Liu et al. 2001) and the range of −12.01‰ to −1.94‰ in Weinan section (Liu et al. 1997).

In general, carbon dioxide in the subsoil or deep soil is produced by biological processes, e.g. heterotrophic oxidation of organic carbon (i.e. microbial respiration) and live root respiration (Andrews and Schlesinger, 2001), and/or probably by chemical processes such as degasification via carbonate precipitation (Walvoord et al. 2005). The Keeling plot shows δ^{13}C-CO$_2$ in this study has a positive relationship with the reversed CO$_2$ concentration (y=3.3877x−23.138; r=0.70, Fig. 7). Herein, the intercept of −23.138‰ in the linear equation accurately equals to the average δ^{13}C of organic carbon in this profile (−23.1‰), consistent with others' results in Chinese Loess Plateau (Zhou et al. 2014; Lu et al. 2015; Yang et al. 2015; Zhou et al. 2016; Lyu et al. 2018). Thus we hypothesize it as one end member of CO$_2$ origin in this profile and $\delta^{13}C_{carb}$=−8 ‰ as the other end-member of soil CO$_2$ according to other' s data (Liu et al. 2011). The data of this study plotted in the Keeling figure is closer to the organic carbon-originated end-member, indicating that the CO$_2$ is mainly derived from biological processes, here, as microbial decomposition of stable organic carbon considering root respiration is little in deep soil.

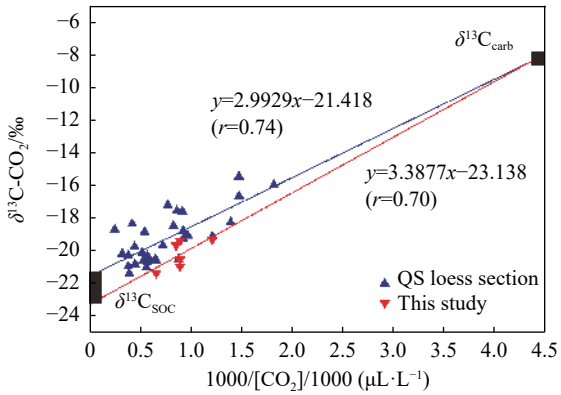

Fig. 7 Inverse of CO$_2$ concentration against isotope signature (Keeling plot)

1/[CO$_2$]= the inverse CO$_2$ concentration; Data of QS loess section are from (Song et al. 2017a); $\delta^{13}C_{carb}$ end member is the mean δ^{13}C of soil carbonate in study area (approximately −8 ‰); $\delta^{13}C_{SOC}$ end member is roughly −22% (−23.1% for this profile and −21.4% for QS section)

The results of SOC and SIC, δ^{13}C of SOC and CO$_2$ at different observation depths are listed in Table 3. In this table, the difference of δ^{13}C between CO$_2$ and soil organic carbon, $\Delta\delta^{13}C=\delta^{13}C_{CO2}-\delta^{13}C_{SOC}$ is increasing with depth (Table 3), indicating more carbonate-derived CO$_2$ components at the bottom of the LTC profile. According to the two end member mixing model, the contribution ratios of SOC and carbonate precipitation to loess CO$_2$ were 74.28%-87.85% (average 80.22%) with an increase followed by a decrease and 12.15%-25.72% (average 19.78%) with a decrease followed by an increase with depths, respectively (Table 3).

Comparing with the QS profile at the depth of 85 m, this LTC profile has a smaller intercept but a steeper slope, a lower δ^{13}C-CO$_2$ in this profile (Fig. 7), and a slightly less contribution of SOC decom-

Table 3 Results of SOC SIC and δ^{13}C at the observed layers and related calculated values

No.	Depth (m)	SOC (%)	SIC (%)	$\delta^{13}C_{SOC}$ (‰)	$\delta^{13}C_{CO2}$(‰)	$\Delta\delta^{13}$C(‰)	$CO_{2\text{-}SOC}$%	$CO_{2\text{-}Carb}$%
LTC1	1.9	0.083	1.911	−22.8	−20.45	2.35	82.48	17.52
LTC2	3.0	0.057	1.745	−22.9	−20.87	2.03	85.21	14.79
LTC3	4.1	0.077	1.842	−23.4	−21.27	2.13	87.85	12.15
LTC4	5.1	0.060	1.086	−23.4	−19.57	3.83	76.62	23.38
LTC5	6.1	0.035	2.361	−23.6	−19.31	4.29	74.89	25.11
LTC6	7.1	0.077	1.129	−23.2	−19.22	3.98	74.28	25.72
	Mean	0.065	1.679	−23.2	−20.11	3.10	80.22	19.78

$\Delta\delta^{13}C=\delta^{13}C_{CO2}-\delta^{13}C_{SOC}$; $CO_{2\text{-}SOC}$: SOC-derived CO$_2$; $CO_{2\text{-}Carb}$: carbonate-derived CO$_2$

position to loess CO_2 (40%-78% with an average of 35%) (Song et al. 2017a), suggesting that CO_2 in the LTC profile has closer relationship with the organic carbon decomposition, especially for the upper three observing depths in this profile. The bigger contribution of carbonate precipitation at the lower section of this profile (23.38%-25.72%) is mainly attributed to the chemical reaction: $Ca^{2+} + HCO_3^- = CaCO_3 + H_2O + CO_2$. When the water in soil evaporates, the CO_2 and the secondary carbonate mineral are produced. The amount of the chemical products mainly depends on the quantity of soil water. That is the reason why the maximum of CO_2 concentration (4 180 $\mu L \cdot L^{-1}$) and the highest contribution ratio of carbonate precipitation (65%) occurs at the bottom of the QS section with high soil water contents (Song et al. 2017a; 2017b). Many studies on soil CO_2 in unsaturated zones with different soil types found the highest CO_2 concentration at the interface between the unsaturated and saturated zone as the result of the attribution of CO_2 degasification of aquifers (Table 4). Despite the small contribution from carbonate precipitation, upward diffusion from depth strongly influences the distribution of CO_2 and carbon isotopes (Walvoord et al. 2005).

4.2 Controlling factors of soil CO_2 concentration and efflux and its responses to excavation

4.2.1 Natural controlling factors: Temperature, soil water, soil properties

According to the above discussion, 80.22% of the CO_2 in the loess of this profile was from microbial decomposition of SOC (biological process) and 19.78% from the degasification during carbonate precipitation (abiotic process). These two processes are controlled by soil temperature and soil moisture (Maier et al. 2011), which is the major reason of the seasonal variation of soil CO_2 at LTC profile in this study as we mentioned in section 4.1. In summer, the warm temperature and ample rainfall are in favor of microbial growth, and promote microbe to break down more organic C in the soil, resulting in high CO_2 concentration. In addition, rain pulses in summer stimulate soil respiration (Liu et al. 2002; Lee et al. 2004; Xiang et al. 2008; Deng et al. 2017) , which also result in an increase in soil CO_2 concentration (Jassal et al. 2005; Flechard et al. 2007; Maier et al. 2010).

However, increases in soil water content do not always enhance both soil surface CO_2 flux and soil CO_2 concentration. Under high soil water conditions, increases in soil water content could lower soil surface CO_2 flux and increase soil CO_2 concentration (Hashimoto and Komatsu, 2006). Elevated litter DOC fluxes could directly stimulate microbial respiration. Many studies have shown that labile C additions such as litter-leached DOC inputs rapidly stimulate microbial growth and CO_2 efflux (Fierer and Schimel, 2003; Cleveland et al. 2007).

Higher soil CO_2 concentration do not always coincide with greater soil surface CO_2 efflux (Hashimoto and Komatsu, 2006). The efflux of CO_2 from the soil to the atmosphere is controlled by diffusion and therefore related to the concentration of CO_2 in the soil atmosphere and the diffusivity of CO_2 in the soil. The diffusion of CO_2 is related to soil bulk density, total porosity and the proportion of macro-pores in the soil (Pengthamkeerati et al. 2005), as well as soil water content (Jassal et al. 2004). These soil physical properties affect its hydraulic properties, which support soil aeration, water and gas transport, and consequently, produce favorable aerobic conditions for soil microorganisms (Pengthamkeerati et al. 2005). Soil CO_2 efflux is more dependent on changes in soil water content than soil temperature (Pengthamkeerati et al. 2005). In this study, the LTC profile has narrow range of grain size distribution as one of the most important properties of windblown mineral dust deposits. Thus bulk density, total porosity and the proportion of macro-pores are not key controlling factors of CO_2 diffusion in this profile except that LTC1 layer may have deep root impact. The observed seasonal change of soil CO_2 efflux in this study: Summer > winter, is not only controlled by the microbial decomposition of SOC, but also impacted by higher soil water content in summer. During evaporation, the CO_2 and H_2O in soil and their efflux to the atmosphere along the section might increase as explained by the following equation: $Ca^{2+} + HCO_3^- = CaCO_3 + H_2O + CO_2$. So the efflux of CO_2 in this study has no distinct relationship with soil CO_2 concentration.

4.2.2 Anthropic perturbation

Higher CO_2 concentrations in the soil pore space reflect increased CO_2 production rates in the soil and create a larger diffusion gradient from the soil to the atmosphere (Andrews and Schlesinger, 2001). In the loess plateau, excavation activities such as terracing practices and engineering constructions for buildings, roads, and tunnels change the CO_2 diffusion and efflux mechanisms. Before excavation, all CO_2 produced in the soil would be

Table 4 Characteristics of soil CO_2 in different unsaturated zone in the world

No.	Location	Thickness of unsaturated Zone	Type of soil	Maximum depth for observation (observation solution)	Characteristics of soil CO_2	Variation of CO_2 concentration with depth	Ref.
1	The U.S. Geological Survey's Amargosa Desert Research Site	110 m	Predominantly sand and gravel (unconsolidated debris flow, fluvial, and alluvial-fan deposits)	110 m;	Maximum: 10^5 μL/L	Increase	(Thorstenson et al. 1998; Walvoord, et al. 2005)
2	Dalmeny site: 30 km northern of Saskatoon, Canada	7.0 m	Clay mainly	6.8 m (0.4, 0.9, 1.7, 3.0, 4.7, 6.8 m)	39 000 μL/L	Increase	(Keller and Bacon, 1998)
3	Rifle site in western Colorado, USA (Experiment site of U.S. Department of Energy (DOE)	3.5 m	Unconsolidated gravel and cobbles interspersed with fine grained silt and clay and locally organic-rich sediments	3.0 m	The maximum is 60 000 μL/L at the depth of 3 m	Increase	(Arora et al. 2016)
4	5 km SE of Delhi, Ontario (Big Creek Drainage Basin)	5.8 m	Medium sand	5.8 m	40 000 μL/L	Increase	(Reardon et al. 1979)
5	Southern Amazon basin: Juruena, Mato Grosso, Brazil (10°25' S; 58°46' W, 230-250 m asl)	8 m	Mosaic of Oxisols and Ultisols (acid soil)	8 m (0.1, 0.25, 0.5, 1, 2, 4, 6, 8 m)	9 000 μL/L	Increase followed by decrease	(Johnson et al. 2008)
6	10 km south of Saskatoon, Canada	6 m	Aeolian sand	6 m (0.30, 0.56, 1.06, 1.56, 2.08, 2.61, 3.13; 4.56; 5.12 m)	400-12 900 μL/L	Decrease in summer; Increase in Winter	(Hendry et al. 1999)
7	Southeast Phoenix, AZ, in the southeastern region of the West Basin of the Salt River Valley	6-9 m	Silty sands and moderately well graded gravels	6 m	The maximum is 30 000 μL/L at the depth of 6 m	Decrease followed by increase	(Suchomel et al. 1990)
8	Cape cod, Southeastern Massachusetts, USA	0.5-12 m	Sands and gravels	3.5 m	Maximum 50 000 μL/L	Increase	(Lee, 1997)
9	Gigante Peninsula (9°06' N, 79°50' W)	2 m	Clay	2 m (0.05, 0.2, 0.4, 0.75, 1.25 and 2 m)	40 000 μL/L	Increase	(Koehler et al. 2010)

emitted through soil surface efflux on a long-term basis (Hashimoto et al. 2007; Maier et al. 2011), but a new vertical profile is commonly developed after excavation, causing an increase in the exposed surface area of soil. In this study, the content of SOC at LTC1 is much lower than that at the surface, but the CO_2 flux at the depth of 1.9 m is relatively high in summer comparing with the surface flux, where 80.22% of the CO_2 is mainly derived from SOC decomposition. This suggests that the vertical profile acts as a new interface for carbon exchange between soil C stock and atmospheric C stock, and soil CO_2 close to the cutting section is prior to emit out laterally and downwardly rather than upwardly, because the upward diffusion of CO_2 in the soil needs to offset the molecular gravity of its own, especially in wet season. According to the flux of CO_2 in Table 2, the average CO_2 flux through vertical cutting profile is 2.47 $g \cdot m^{-2} \cdot d^{-1}$, equaling to 23.89% of that from the surface (10.34 $g \cdot m^{-2} \cdot d^{-1}$). The proportion is consistent with the regional estimation on the ratio of from back wall to the CO_2 flux at the surface (approximately 20%) due to the terrace practice in Qiushe area (Song, 2017).

4.3 The SOC decomposition due to excavation and its implication to soil carbon management

Soil organic carbon in loess is a huge carbon pool, preserving organic carbon as old as millions of years. The preservation mechanisms of organic carbon are mainly physical adsorption and chemisorption by ligand exchange of kaolinite， and complexation of iron (Fe_p) and sorption of amorphous oxides of iron (Fe_o) (Wang et al. 2013). The annual variation trend of soil CO_2 indicates that these old carbon stored in deep loess can be exposed and subsequently decomposed by microbes in 1-2 years after excavation, which is consistent with the study on the terracing practice (Chen et al. 2020). Chen et al. (2020) summarized about 78 studies regarding terracing effects on SOC sequestration and concluded that in terracing practices, topsoil removals exposed the previously preserved SOC, causing an average decrease of 6.4% on SOC sequestration in the youngest terraces with age of 1-2 years, probably because the breakdown of soil aggregates through soil excavation and redistribution improves the decomposition of SOC (Chen et al. 2020; Liu et al. 2020). Although terracing aged over five years increased SOC sequestration by 32.4% on average in China's landscapes, yet the prerequisites are that the C-unsaturated soil that is exposed during terracing cutting has proper climatic and structural conditions to accumulate OC.

The study also showed that land use type, age of terracing, climatic background, and slope gradient were critical factors for SOC sequestration in terracing, while terracing structure and soil depth were less important (Chen, et al. 2020). Nevertheless, the subsurface soil exposed by the engineering constructions for building and road was commonly covered by the cement and/or concrete, and bitumen, sealing the preservation of potential organic carbon. Thus, the decrease or increase of SOC is mainly controlled by the treatment mode of the fresh C-unsaturated soil. Terracing in the areas with lower temperatures and less precipitation showed higher SOC sequestration. But the extent of SOC sequestration due to terracing was primarily determined by land use type (Chen et al. 2020).

5 Conclusions

The characteristics of CO_2 concentration on a newly-excavated loess profile in the central CLP was observed for seven years. The results showed that the CO_2 concentrations decrease with both depth and time. 80.22% of these CO_2 is from microbial decomposition of SOC and 19.78% from the degasification during carbonate precipitation according to $\delta^{13}C$-CO_2 calculation. Our findings revealed human excavation can lead to the increase of CO_2 concentrations within the first two years after excavation, which subsequently decrease to the normal value as observed from other natural loess profiles. Moreover, our results suggest that the new vertical profile after human excavation acts as an important interface for carbon exchange as the lateral CO_2 efflux between soil C stock (including SOC and SIC stock) and atmospheric C stock. These results can help to better understand the loess carbon models under the impacts of human activities (excavation, terracing practices, bulldozing mountains to build cities, etc) and develop techniques for enhancing C sequestration in loess

Acknowledgements

This research was funded by National Natural Science Foundation of China (Grant No. 41877 398), the Basic Science Research Fund from the Institute of Chinese Academy of Geological Sciences (Grant No. SK201911), and the Belt and

Road Fund on Water and Sustainability (U2019-NKMS01). We give many thanks to Prof. Cornelia Rumpel from Institute of Ecology and Environmental Sciences Paris and two anonymous reviewers, who provided many invaluable suggestions for revising this paper.

References

Andrews JA, Schlesinger WH. 2001. Soil CO_2 dynamics, acidification, and chemical weathering in a temperate forest with experimental CO_2 enrichment. Global Biogeochemical Cycles, 15(1): 149-162.

Arora B, Spycher NF, Steefel CI, et al. 2016. Influence of hydrological, biogeochemical and temperature transients on subsurface carbon fluxes in a flood plain environment. Biogeochemistry, 127(2-3): 367-396.

Capaccioni B, Caramiello C, Tatàno F, et al. 2011. Effects of a temporary HDPE cover on landfill gas emissions: Multiyear evaluation with the static chamber approach at an Italian landfill. Waste Management, 31(5): 956-965.

Chaopricha NT, Marín-Spiotta E. 2014. Soil burial contributes to deep soil organic carbon storage. Soil Biology and Biochemistry, 69: 251-264.

Chen D, Wei W, Daryanto S, Tarolli P. 2020. Does terracing enhance soil organic carbon sequestration? A national-scale data analysis in China. Science of the Total Environment, 721: 137751.

Chen Q, Shen C, Sun Y, et al. 2007. Characteristics of soil organic carbon and its isotopic compositions. Chinese Journal of Ecology, 26(9): 1327-1334.

Cleveland CC, Nemergut DR, Schmidt SK, et al. 2007. Increases in soil respiration following labile carbon additions linked to rapid shifts in soil microbial community composition. Biogeochemistry, 82(3): 229-240.

Deng Q, Hui D, Chu G, et al. 2017. Rain-induced changes in soil CO_2 flux and microbial community composition in a tropical forest of China. Scientific Reports, 7(1): 5539.

Etiope G. 1999. Subsoil CO_2 and CH_4 and their advective transfer from faulted grassland to the atmosphere. Journal of Geophysical Research:Atmospheres, 104(D14): 16889-16894.

Fierer N, Schimel JP. 2003. A proposed mechanism for the pulse in carbon dioxide production commonly observed following the rapid rewetting of a dry soil. Soil Science Society of America Journal, 67(3): 798-805.

Flechard CR, Neftel A, Jocher M, et al. 2007. Temporal changes in soil pore space CO_2 concentration and storage under permanent grassland. Agricultural and Forest Meteorology, 142(1): 66-84.

Fontaine S, Barot S, Barré P, et al. 2007. Stability of organic carbon in deep soil layers controlled by fresh carbon supply. Nature, 450(7167): 277-280.

Gao Y, Tian J, Pang Y, et al. 2017. Soil inorganic carbon sequestration following afforestation is probably induced by pedogenic carbonate formation in Northwest China. Frontiers in Plant Science, 8: 1282.

Gerke H, Rieckh H, Sommer M. 2015. Interactions between crop, water, and dissolved organic and inorganic carbon in a hummocky landscape with erosion-affected pedogenesis. Soil and Tillage Research, 156: 230-244.

Granieri D, Chiodini G, Marzocchi W, et al. 2003. Continuous monitoring of CO_2 soil diffuse degassing at Phlegraean Fields (Italy): Influence of environmental and volcanic parameters. Earth and Planetary Science Letters, 212(1-2): 167-179.

Han G, Yang T, Man L, et al. 2020. Carbon-nitrogen isotope coupling of soil organic matter in a karst region under land use change, Southwest China. Agriculture Ecosystems & Environment, 301: 107027.

Hashimoto S, Komatsu H. 2006. Relationships between soil CO_2 concentration and CO_2 production, temperature, water content, and gas diffusivity: implications for field studies through sensitivity analyses. Journal of Forest Research, 11(1): 41-50.

Hashimoto S, Tanaka N, Kume T, et al. 2007. Seasonality of vertically partitioned soil CO_2 production in temperate and tropical forest. Journal of Forest Research, 12(3): 209-221.

Hendry MJ, Mendoza CA, Kirkland RA, et al. 1999. Quantification of transient CO_2 production in a sandy unsaturated zone. Water Re-

sour. Res, 35(7): 2189-2198.

IPCC. 2018. Global Warming of 1.5℃: An IPCC Special Report on the impacts of global warming of 1.5℃ above pre-industrial levels and related global greenhouse gas emission pathways, in the context of strengthening the global response to the threat of climate change, sustainable development, and efforts to eradicate poverty.

IPCC. 2021. Climate Change 2021: The Physical Science Basis. Contribution of Working Group I to the Sixth Assessment Report of the Intergovernmental Panel on Climate Change. In: Masson-Delmotte V, Zhai P, Pirani A, et al.

Jassal R, Black A, Novak M, et al. 2005. Relationship between soil CO_2 concentrations and forest-floor CO_2 effluxes. Agricultural and Forest Meteorology, 130: 176-192.

Jassal RS, Black TA, Drewitt GB, et al. 2004. A model of the production and transport of CO_2 in soil: Predicting soil CO_2 concentrations and CO_2 efflux from a forest floor. Agricultural and Forest Meteorology, 124(3-4): 219-236.

Jobbágy E, Jackson R. 2000. The vertical distribution of soil organic carbon and its relation to climate and vegetation. Ecological Applications, 10(2): 423-436.

Johnson MS, Lehmann J, Riha SJ, et al. 2008. CO_2 efflux from Amazonian headwater streams represents a significant fate for deep soil respiration. Geophysical Research Letters, 35(L17401): 1-5.

Keller CK, Bacon DH. 1998. Soil respiration and georespiration distinguished by transport analyses of vadose CO_2, $^{13}CO_2$, and $^{14}CO_2$. Global Biogeochemical Cycles, 12(2): 361-372.

Koehler B, Zehe E, Corre MD, et al. 2010. An inverse analysis reveals limitations of the soil-CO_2 profile method to calculate CO_2 production and efflux for well-structured soils. Biogeosciences, 7: 2311-2325.

Lal R. 2004. Soil carbon sequestration impacts on global climate change and food security. Science, 304: 1623-1627.

Lee RW. 1997. Effects of carbon dioxide variations in the unsaturated zone on water chemistry in a glacial-outwash aquifer. Applied Geochemistry, 12(4): 347-366.

Lee X, Wu H, Sigler J, et al. 2004. Rapid and transient response of soil respiration to rain. Global Change Biology, 10: 1017-1026.

Liegler A. 2016. Diffuse CO_2 degassing and the origin of volcanic gas variability from Rincón de la Vieja, Miravalles and Tenorio Volcanoes, Guanacaste Province, Costa Rica. M. S. thesis. Houghton, Michigan: Michigan Technological University: 1-69.

Liu J, Han G. 2020. Effects of chemical weathering and CO_2 outgassing on $\delta^{13}C$ DIC signals in a karst watershed. Journal of Hydrology, 589: 125192.

Liu J, Hua Z, Liu D. 1997. Preliminary study of greenhouse gases in loess in Weinan, Shaanxi Province. Chinese Science Bulletin, 42(11): 921-924.

Liu M, Han G, Li X. 2021. Comparative analysis of soil nutrients under different land-use types in the Mun River basin of Northeast Thailand. Journal of Soils and Sediments(21): 1136-1150.

Liu M, Han G, Zhang Q. 2020. Effects of agricultural abandonment on soil aggregation, soil organic carbon storage and stabilization: Results from observation in a small karst catchment, Southwest China. Agriculture, Ecosystems & Environment, 288: 106719.

Liu Q, Liu J, Sui S. 2001. Features of major greenhouse gases in loess, Shanxi Province, China. Chinese Science Bulletin, 46(17): 1469-1471.

Liu T. 1985. Loess and the Environment. Beijing: China Ocean Press. 1-481. (In Chinese)

Liu W, Yang H, Ning Y, et al. 2007. Contribution of inherent organic carbon to the bulk $\delta^{13}C$ signal in loess deposits from the arid western Chinese Loess Plateau. Organic Geochemistry, 38(9): 1571-1579.

Liu W, Yang H, Sun Y, et al. 2011. $\delta^{13}C$ Values of loess total carbonate: A sensitive proxy for Asian summer monsoon in arid northwestern margin of the Chinese loess plateau. Chemical Geology, 3-4(284): 317-322.

Liu X, Wan S, Su B, et al. 2002. Response of soil CO_2 efflux to water manipulation in a tallgrass prairie ecosystem. Plant and Soil, 240(2): 213-223.

Liu Z. 2011. Is pedogenic carbonate an important atmospheric CO_2 sink? Chinese Science Bul-

letin, 56(35): 3794-3796. https://doi.org/10.1007/s11434-010-4288-8

Lu H, Hongyan Z, Lin Z, et al. 2015. Temperature forced vegetation varations in glacial interglacial cycles in northeastern China revealed by loess palesol deposit. Quaternary Sciences, 35(4): 828-836.

Lyu A, Lu H, Lin Z, et al. 2018. Variation and possible forcing mechanism of organic carbon isotopic compositions of loess in Northeastern China over the past 1. 08 Ma. Journal of Asian Earth Sciences, 155: 174-179.

Maier M, Schack-Kirchner H, Hildebrand EE, et al. 2010. Pore-space CO_2 dynamics in a deep, well-aerated soil. European Journal of Soil Science, 61(6): 877-887.

Maier M, Schack-Kirchner H, Hildebrand EE, et al. 2011. Soil CO_2 efflux vs. soil respiration: Implications for flux models. Agricultural & Forest Meteorology, 151(12): 1723-1730.

Pabst H, Gerschlauer F, Kiese R, et al. 2016. Land use and precipitation affect organic and microbial carbon stocks and the specific metabolic quotient in soils of eleven ecosystems of Mt. Kilimanjaro, Tanzania. Land Degradation & Development, 27(3): 592-602.

Pengthamkeerati P, Motavalli PP, Kremer RJ, et al. 2005. Soil carbon dioxide efflux from a claypan soil affected by surface compaction and applications of poultry litter. Agriculture, Ecosystems and Environment, 109(1): 75-86.

Popiţa G, Frunzeti N, Ionescu A, et al. 2015. Evaluation of carbon dioxide and methane emission from Cluj-Napoca municipal landfill, Romania. Environmental Engineering and Management Journal, 14(6): 1389-1398.

Qin XG, Li CS, Cai BG. 2001. The sensitivity simulation of climate impact on C pools of loess. Quaternary Sciences, 21(2): 153-161.

Reardon EJ, Allison GB, Fritz P. 1979. Seasonal chemical and isotopic variations of soil CO_2 at Trout Creek, Ontario. Journal of Hydrology, 43(1): 355-371.

Song C, Han G, Ning Z, et al. 2017a. The characteristics and origin of CO_2 in unsaturated zone at loess tableland of Northwestern China. Quaternary Research, 37(6): 1172-1181.

Song C, Han G, Shi Y, et al. 2017b. Characteristics of CO_2 in unsaturated zone(~90 m) of loess tableland, Northwest China. Acta Geochimica, 36(3): 489-493.

Song C. 2017. Characteristics and origin of soil CO_2 at unsaturated zone in loess tableland and its implication to carbon cycle. Ph. D. thesis. Beijing: China University of Geosciences (Beijing): 1-132. (In Chinese)

Suchomel KH, Kreamer DK, Long A. 1990. Production and transport of carbon dioxide in a contaminated vadose zone: a stable and radioactive carbon isotope study. Environmental science & technology, 24(12): 1824-1831.

Tan W, Zhang R, Cao H, et al. 2014. Soil inorganic carbon stock under different soil types and land uses on the Loess Plateau region of China. Catena, 121: 22-30.

Thorstenson DC, Weeks EP, Haas H, et al. 1998. Chemistry of unsaturated zone gases sampled in open boreholes at the crest of Yucca Mountain, Nevada: Data and basic concepts of chemical and physical processes in the mountain. Water resources research, 34(6): 1507-1529.

Walvoord MA, Striegl RG, Prudic DE, et al. 2005. CO_2 dynamics in the Amargosa Desert: Fluxes and isotopic speciation in a deep unsaturated zone. Water resources research, 41(2): W02006.

Wang C, Li F, Shi H, et al. 2013. The significant role of inorganic matters in preservation and stability of soil organic carbon in the Baoji and Luochuan loess/paleosol profiles, Central China. Catena, 109: 186-194.

Wang JP, Wang XJ, Zhang J, et al. 2015. Soil organic and inorganic carbon and stable carbon isotopes in the Yanqi Basin of northwestern China. European Journal of Soil Science, 66(1): 95-103.

Wood WW, Petraitis MJ. 1984. Origin and distribution of carbon dioxide in the unsaturated zone of the southern high plains of Texas. Water Resources Research, 20(9): 1193-1208.

Xiang SR, Doyle A, Holden PA, et al. 2008. Drying and rewetting effects on C and N mineralization and microbial activity in surface and subsurface California grassland soils. Soil Biology and Biochemistry, 40(9): 2281-2289.

Yang S, Ding Z, Li Y, et al. 2015. Warming-induced northwestward migration of the East

Asian monsoon rain belt from the Last Glacial Maximum to the mid-Holocene. Proceedings of the National Academy of Sciences of the United States of America, 112(43): 13183.

Zamanian K, Pustovoytov K, Kuzyakov Y. 2016. Pedogenic carbonates: Forms and formation processes. Earth Science Reviews, 157: 1-17.

Zamanian K, Zarebanadkouki M, Kuzyakov Y. 2018. Nitrogen fertilization raises CO_2 efflux from inorganic carbon: A global assessment. Global Change Biology, (24): 2810-2817.

Zhou B, Shen C, Sun W, et al. 2014. Late Pliocene-Pleistocene expansion of C_4 vegetation in semiarid East Asia linked to increased burning. Geology, 42(12): 1067-1070.

Zhou B, Wali G, Peterse F, et al. 2016. Organic carbon isotope and molecular fossil records of vegetation evolution in central Loess Plateau since 450 kyr. Science China, 59(6): 1206-1215.